Available online at www.sciencedirect.com

ScienceDirect

Procedia Engineering 2 (2010) 407–416

Procedia Engineering

www.elsevier.com/locate/procedia

Fatigue 2010

Investigations of the effect of creep fatigue interaction in a Cu-Cr-Zr alloy

Pierre Marmy[a]*, Olivier Gillia[b]

[a]SCK.CEN, RTD, Boeretang 200, 2400 Mol, Belgium
[b]CEA, DRT/LITEN, 17 rue des Martyrs, 38054 Grenoble, France

Received 5 March 2010; revised 9 March 2010; accepted 15 March 2010

Abstract

The low cycle fatigue, the creep and the creep-fatigue properties of Cu-Cr-Zr have been investigated at 300 °C. The material investigated is an ELBRODUR G, heat treated to the following condition: 980°C-30 min, ageing 580°C-2 hours. This condition corresponds to a possible fabrication and heat treatment route of the first wall blanket panels of the ITER fusion reactor. The microstructure is characterized by a coarse grain size, with grains reaching sizes up to 500 µm. Curves and equations describing the creep and the fatigue properties have been obtained. A few creep-fatigue experiments have been conducted for tensile dwells of 30 and 300 sec. The results have been analyzed according to the time based life assessment method. The results indicate that fatigue and creep damage are not simply additive but a strong interaction takes place, especially at low imposed strains. Two damage envelopes for 30 and 300 sec have been determined. They can be used for making predictions between close experimental points.

Keywords: creep; fatigue; creep-fatigue; copper alloys

1. Introduction

Cu-Cr-Zr alloy is a primary candidate material for the heat sinks at the first wall of the ITER fusion reactor. The blanket modules in which Cu-Cr-Zr will serve as an heat extracting material are subjected to thermal fatigue at a temperature around 300°C. Cu-Cr-Zr is submitted to stresses because of temperature gradients and coefficient of thermal expansion mismatch with the materials to which it is assembled in the first wall panels (AISI 316LN and beryllium tiles). This loading situation was only studied once under ITER conditions by Bretherton [1]. The results indicate a strong reduction of fatigue life in the presence of 5 min tensile dwells, especially at low imposed strains. Basically creep fatigue consists of applying a pre-defined load during a fixed period followed by a full load reversal and re-loading to the initial value. It is of prime importance to check how the damage received under the constant load (creep) will change the sensitivity of the material to the damage sustained during the load reversal and re-loading (fatigue) and vice-versa. This interaction between fatigue and creep is very large in Cu-Cr-Zr and takes place even at room temperature [2]. The phenomenon has not been completely elucidated up to now. A series of

* Corresponding author. Tel.: +32-14 33 34 53; fax: +32-14 32 13 36.
E-mail address: pierre.marmy@sckcen.be.

1877-7058
doi:10.1016/j.proeng.2010.03.045

creep, fatigue and creep fatigue tests has been conducted with an over aged material, as it is potentially used in ITER. The creep fatigue results are then analyzed in the light of a time based damage assessment model. This approach gives a different perspective for the understanding of the creep fatigue interaction. The damage model is proposed to obtain prediction rules to assess creep fatigue performance out of isolated creep and fatigue results.

2. Experimental

The material ELBRODUR G of this study is a product of the company KME. The batch designation given to the alloy by KME is Cu-Cr-Zr 92. The chemical analysis in wt % is as follows (Table 1):

Table 1. Chemical analysis of the Elbrodur G, Cu-Cr-Zr 92 alloy.

Cr	Zr	Cu	Fe	Sb	Si	P
0.84	0.138	98.97	0.024	0.004	0.003	0.021

The material has been delivered in the form of a 30 mm plate. Normally the material receives a solution annealing followed by an aging according to: 30 min at 975°C, water quenched, 2-4 hours at 475°C, water quenched. The material of this study was heat treated according to the fabrication route of the ITER modules:

Solutioning: 980°C- 30 min, cooling rate 50-60°C/min
Ageing : 580°C – 2 hours

In order to expedite the testing, equipments from two laboratories were engaged. The fatigue testing was done using two systems, a RMC100 test machine and a MTS servo hydraulic frame. Both series of tests were run in vacuum, controlling the strain by an extensometer equipped with ceramic rods applied on the gauge length of the specimen. The tensile tests were accomplished in vacuum, in the MTS test frame. The creep tests were done using two different machines. The first one was a stress constant loading system based on mechanical cams. The specimen was placed into a resistive furnace constantly flushed with argon. The second system was a four post test machine in which four specimens were loaded in a single vacuum furnace. The load acting on each specimen was constant. In both systems, inspections after the test indicated that the samples were not oxidized during their exposure in the furnace.

Four different specimen geometries have been used. For the tensile and the creep tests in the four post machine, cylindrical specimens having a 30 mm gauge length and 6 mm diameter were used. The specimens used in the MTS system for fatigue and creep fatigue, had a diameter of 9 mm and a gauge length of 18 mm. The specimens used in the RMC 100 for fatigue and creep fatigue had a diameter of 3 mm and a gauge length of 6 mm. Finally the specimens used in the constant stress creep machine had a diameter of 6 mm and a gauge length of 20 mm. All specimens for fatigue and creep deformation were cut in the longitudinal direction of the plate. The orientation according to ASTM is L-T, specimen axis in the length direction and main plane for crack propagation in the transverse direction.

The tests were all carried out at 300°C. The applied strain rate during the tensile tests was 10^{-4} s^{-1}. All fatigue and creep fatigue tests were conducted with a strain rate of $3x10^{-3}$ s^{-1}. Tensile holds of 30 or 300 sec were applied in the creep fatigue tests. The criterion used for determining the number of cycles to failure of the 9 mm specimen was similar to the one described earlier in a work on ferritic martensitic steels [3].

3. Microstructure

The Cu-Cr-Zr Elbrodur G is a precipitation strengthened alloy. Strengthening arises by the addition of second phase small particles in the matrix material. Cu-Cr-Zr contains a high density of nanometre sized particles which mainly control the strength and a lower density of larger size particles which act as barriers for grain growth. The peak strength is obtained after aging at temperatures around 450°C. The material of this study is over aged and the coherency of the precipitates is lost. The strength is decreased as a result of the precipitation of coarse Cr and Cu5Zr

precipitates (see Table 2)[4]. The microstructure has been analyzed with optical microscopy. The grain size obtained is coarse. Most grains have dimensions between 100 and 250 µm while a few reach 500 µm. The grain size obtained is larger as compared to the as received size which is between 50 and 150 µm.

4. Mechanical tests results

4.1. Tensile properties

The tensile properties after the heat treatment are given in the table 2 below, together with the *as received* properties as indicated by the manufacturer. Following the over aging treatment, the yield strength is reduced by 36% while the ultimate strength is decreased by 28%.

Table 2. Tensile properties of the Cu-Cr-Zr 92 alloy in the *as received* and after the heat treatment.

	YS	UTS	A
	MPa	MPa	%
As received	281	417	27
Heat treated	179	302	26

4.2 Creep results

Stress and load constant creep tests on the over aged Cu-Cr-Zr have been conducted at 300°C, using nominal stresses slightly greater than the yield stress. The endurance data are plotted in figure 1 (a). The constant stress data are well aligned on the mean line whereas the constant load data are more scattered. The creep rate never stabilizes to a constant value. Instead the creep crate continuously decreases all over the test until it increases for the final creep stage. Fig. 1 (b) shows the secondary creep rates taken as the minimum creep rate measured during the test. The data point at 190 MPa has been duplicated for a higher temperature of 350°C. As a result, the creep rate was enhanced by a factor 2.6. Since most data are for a single temperature a representation according to Larson-Miller is not appropriate. Instead the data can be described with the following power function:

$$\sigma = 217.27 \cdot t_f^{-0.01693} \tag{1}$$

where σ is the initial stress in MPa and t_f the time to rupture in hours. This relation is only valid in the interval 185 to 212 MPa. To allow for better numerical calculation, the reciprocal fit of the data has been done:

$$t_f = 10^{117.03552} \cdot \sigma^{-49.90504} \tag{2}$$

4.3 Fatigue and creep fatigue results

The general cyclic stress behaviour of the over aged Cu-Cr-Zr is shown in figure 2(a). During the first cycles there is a rapid increase of the flow stress. This increase is significant, reaching values of 4 to 15%, depending on the imposed strain. The increase lasts only for a few cycles, reaches some peak value and then a reverse behaviour with a rapid decrease of the flow stress is observed. At low imposed strain, the decrease of the flow stress is not very apparent. After this initial stress excursion response, the material stabilizes and reaches a saturation state characterized by a slow softening rate. The initial stress cyclic hardening is only partially recovered by the steady state softening. At high imposed strains, the peak stress is reached very early in life whereas at low strains approximately 300 cycles are necessary to reach the saturated state. The plastic strain shows the reverse behaviour. As the cyclic stress increases rapidly, a sharp decrease of the plastic strain is observed. Then the plastic strain increases again as the cyclic stress decreases (see Fig. 2(a) where the total stress is the sum of the absolute positive and negative stresses).

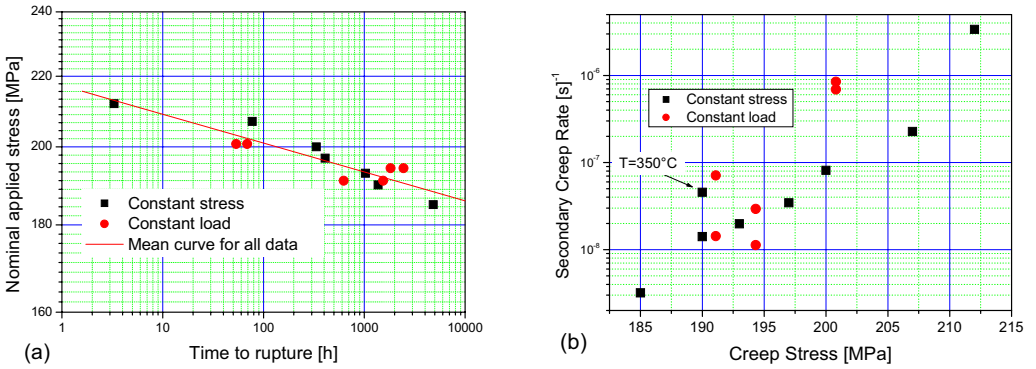

Fig.1. (a) Time to rupture of over aged Cu-Cr-Zr at 300°C; (b) Secondary creep rates as a function of the stress.

Figure 2(b) compares the cyclic stress responses at 0.4 and 0.8% total imposed strain, for continuous fatigue and tests with 30 and 300 sec tensile hold times. Tested at the same strain level, the cyclic stress is nearly not influenced by the presence of the hold times. The number of cycles to failure is clearly reduced by the introduction of the hold times, the effect being larger for the longer dwells and more pronounced at low imposed strains. The fatigue life reduction factor is of the order of 2 for 30 sec tensile hold times. For 300 sec tensile dwells, the life reduction factor is about 2.5 at high strains and reaches 6 at low strains.

The introduction of a tensile hold period in the fatigue cycle broadens the hysteresis loop. Figure 3 shows the resulting plastic strain loops (N= 10000) for continuous fatigue, 30 and 300 sec hold times, together with the loop from a specimen tested at a slightly higher plastic strain but without hold time. The specimen with the larger loop fatigued at 0.65% without hold time lasted longer than the specimen fatigued at 0.41% with a 300 sec tensile hold time.

The fatigue performance of the over aged Cu-Cr-Zr is shown on figure 4 (a) for the 3 mm specimens, according to a Coffin-Manson analysis and in figure 4 (b) for all specimens according to Langer. To demonstrate the effect of the temperature, two tests without hold times have been done at 400 °C. Besides the loss of the mechanical strength, a drastic loss in fatigue life is also observed, as the number of cycles to failure is decreased by a factor 4 (see Fig. 4(a)).

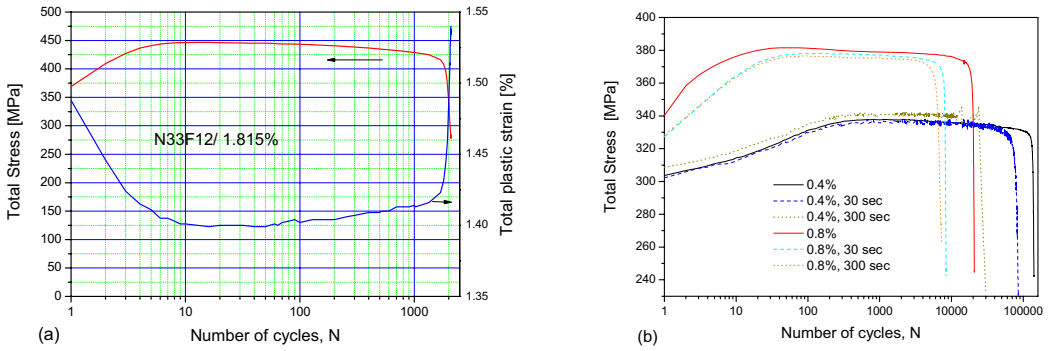

Fig. 2. (a) Typical stress over cycle behaviour observed in over aged Cu-Cr-Zr; (b) Set of cyclic stress curves at 0.4 and 0.8% imposed total strains with and without hold times. Testing at 300°C.

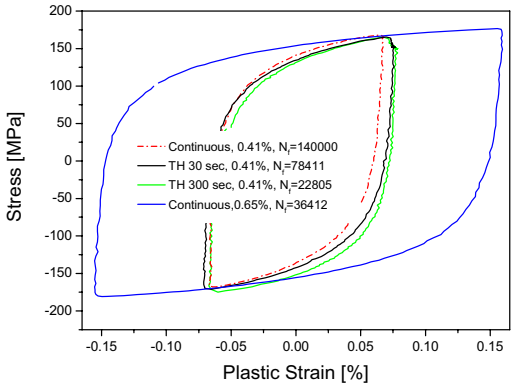

Fig. 3. Stress-plastic strain hysteresis loops for Cu-Cr-Zr specimens fatigued at a $\Delta\varepsilon_t$ =0.41% with and without hold times and $\Delta\varepsilon_t$ =0.65% , at 300°C. The associated number of cycles to failure is indicated. N= 10000.

Continuous fatigue life endurance data shown in figure 5 (a) can be represented using the Coffin-Manson method:

$$\Delta\varepsilon / 2 = 0.36012 \cdot N_f^{-0.0812} + 30.968 \cdot N_f^{-0.50486} \tag{3}$$

Where $\Delta\varepsilon$ is the imposed strain range, the first term is the elastic contribution and the second term the plastic contribution. The transition life (N_f when $\Delta\varepsilon_p/2 = \Delta\varepsilon_e/2$) is at around 35000 cycles. For further data analysis a more simple fatigue life equation is required. The most useful equation is the Langer equation $\Delta\varepsilon_t = A + B \cdot N_f^C$, because it is not connected to the physical mechanisms and contains only dimensionless parameters. The evaluation of the parameters leads to the following relation:

$$\Delta\varepsilon_t = 0.3 + 73.121 \cdot N_f^{-0.5294} \tag{4}$$

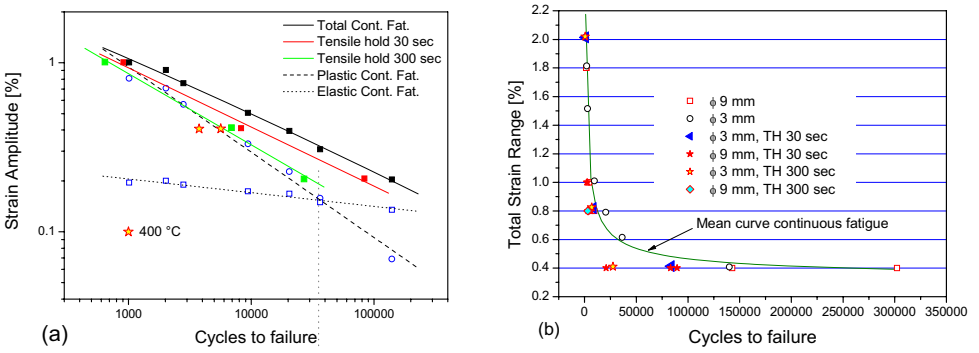

Fig. 4. (a) Coffin-Manson analysis of the 3 mm specimen; (b) Langer plot of all fatigue and creep-fatigue data.

4.4 Stress relaxations during dwells

When the imposed strain rate is not reversed at the top of the hysteresis loop, the stress decreases sharply due to dislocation glide induced plastic flow. Typical relaxations observed at 300 °C at low and high strains are shown in figure 5 (a), for 30 and 300 sec dwells. The relaxations at high strain show a behavior with a constantly decreasing

stress value, whereas the relaxations at low strains are more irregular. The amplitude of the relaxations was found to be relatively high for all cases. The value was of the order of 10% of the stress amplitude. It was not very much dependent on the applied conditions at moderate and high strains. At low strains the relaxation amplitude was clearly lower. It was also observed that the amplitude of the relaxation was slightly increasing over the first cycles but then did not vary up to the initiation of the main crack (see Fig. 5 (b)). The following two equations describe the relaxed stress amplitude as a function of the imposed total strain (0.4-2%), as observed in our testing at 300°C:

For 300 sec dwells:

$$\Delta\sigma_{relax} = 7.37 + 22.45 \cdot \Delta\varepsilon_t - 5.54 \cdot \Delta\varepsilon_t^2 \tag{5}$$

For 30 sec dwells:

$$\Delta\sigma_{relax} = 0.68 + 46.08 \cdot \Delta\varepsilon_t - 28.32 \cdot \Delta\varepsilon_t^2 + 5.68 \cdot \Delta\varepsilon_t^3 \tag{6}$$

The analysis of the plotted relaxations at first cycle and at half life indicates that the relaxations obey similar time dependencies and are homothetic. The stress relaxation behaviour of the Cu-Cr-Zr near half life can be described using a modified Feltham approach [5, 6]:

$$\sigma_{Relax}(t) = a_1 \cdot \ln(a_2 \cdot t + a_3) \tag{7}$$

The fit is generally quite good. The parameter a_1, a_2 and a_3 for the different load cases have been listed in table 3 below:

Table 3. Fitting parameters of relaxations

$\Delta\varepsilon_t$ [%]	Dwell [sec]	a1	a2	a3
0.413	30	-1.60274	472.66154	0.83932
0.82	30	-3.16306	78.51938	0.64231
2.014	30	-3.14839	79.74906	0.75424
0.41	300	-1.17231	1101.18201	2.2161
0.825	300	-2.01296	356.95333	0.7757
2.02	300	-2.96515	118.18966	0.64705

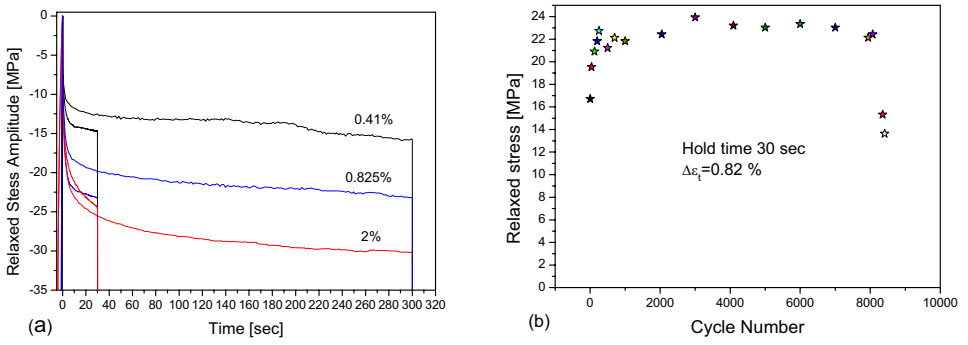

Fig. 5. (a) Stress relaxations in Cu-Cr-Zr at 300°C; (b) Typical behaviour of the amplitude of the relaxed stress as a function of the cycle number

4.5 Cyclic stress behaviour

Assuming the material is obeying a relation of the type $\Delta\sigma = K \cdot \Delta\varepsilon_p^{\,n}$, the Ramberg-Osgood equation can be used to predict the total cyclic stress as a function of the applied total strain range Δεt:

$$\Delta\varepsilon_t = \frac{\Delta\sigma}{E} + \left(\frac{\Delta\sigma}{K}\right)^{\frac{1}{n}} \tag{8}$$

where E is the Young's modulus, *n* the plastic hardening exponent and K a constant. The parameters have been determined at half life, where the material is considered to have reached a steady state. The Young's modulus determined as an average of the hysteresis loops taken near half life, has a value of 105 GPa. Figure 6 (a) represents the cyclic stress response of the Cu-Cr-Zr fatigue specimens measured in this study. It can be seen that the values from the experiments with hold times and the values from continuous fatigue show identical dispersion to the mean line. Therefore a single Ramberg-Osgood relation is enough for the data representation:

$$\Delta\varepsilon_t = \frac{\Delta\sigma}{105000} + \left(\frac{\Delta\sigma}{720}\right)^{\frac{1}{0.12}} \tag{9}$$

Since this equation cannot be resolved for Δσ, a reciprocal relation has been determined graphically on the base of an allometric fit. The equation representing the data reads:

$$\Delta\sigma = 634.02 - 61.556 \cdot \Delta\varepsilon_t^{-0.29708} \tag{10}$$

5. Life assessment model

5.1. Damage model

The model presented here is based on estimating simultaneously the damage components from creep and fatigue in terms of percentage of rupture life consumed [7]. The creep damage component will be assessed based on the time spent at different stress levels during each fatigue cycle relaxation.

For the case of monotonic fatigue with holding times, the equation combining fatigue and creep damage is:

$$n \cdot (d_f + d_c) = D \tag{11}$$

where *n* is the number of allowable cycles to reach failure and d_f and d_c are the fatigue and creep damage per cycle.

$$d_f = \frac{1}{N_f} \tag{12}$$

$$d_c = \sum_{k=1}^{m}\left(\frac{\Delta t_k}{T_{rk}(\sigma_k)}\right) \tag{13}$$

N_f is the number of cycles to failure in monotonic fatigue
Δt_k is the creep time at stress σ_k during relaxation
T_{rk} is the rupture time for stress *k*

According to equation (12), the fractional damage due to fatigue and the fractional damage due to creep are summed to give the total damage D at fracture. A value other than 1 for D will imply an interaction between fatigue and creep. How the life reduction occurs is schematically represented in the damage diagram of figure (6) b.

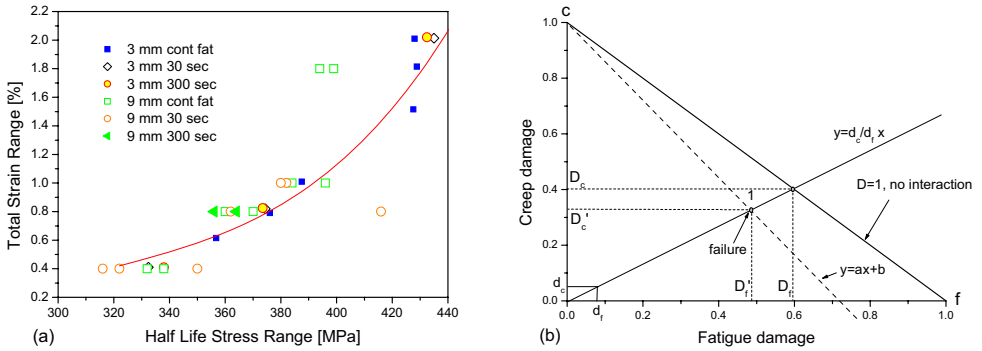

Fig. 6. (a) Cyclic stress strain curve according to Ramberg-Osgood approach; (b) Damage diagram. Point 1 represents a point of the damage boundary for a particular damage ratio d_c/d_f. d_c is the creep damage per cycle and d_f the fatigue damage per cycle. The allowable fatigue damage has been reduced from D_f to D_f'.

For a particular test with a damage partition equal to $\alpha = d_c/d_f$, the intersection with the boundary line y=ax+b is at x=b/(α-a). The number of allowable cycles can be calculated as:

$$n = \frac{b}{d_f(\alpha - a)} \tag{14}$$

and the corresponding value for D is from equation (11):

$$D = \frac{b(d_f + d_c)}{d_f(\alpha - a)} \tag{15}$$

and knowing n from experiment, for the line y=ax+b, we can calculate the slope:

$$a = \alpha - \frac{b}{d_f \cdot n} \tag{16}$$

5.2. Damage evaluation

The evaluation of the fatigue damage is based on the fatigue master curve shown in figure 4(b) and the number of cycles to failure is calculated from the Langer equation (4), for the required imposed total strain range.

The evaluation of the creep damage is more complex and necessitates a few steps. The stress amplitude at half life is determined by taking half of the value given by equation (10) or alternatively when available the value given by the experiment. The associated maximum relaxed stress at half life is found for the general case from relation (5) for 300 sec dwells or (6) for 30 sec dwells. Alternatively, this value can also be obtained for the particular tests from equation (7), using the listed parameters of table 3. The evaluation of equation (13) is done in time intervals of different duration. Each relaxation has been partitioned to 12 intervals in the following way:

- 5 intervals of 6 seconds for the first 30 sec
- 2 intervals of 15 sec up to the end of the first minute of relaxation
- 2 intervals of 30 sec for the second minute of relaxation
- 3 intervals of 1 min to the end of the relaxation.

The mean relaxed stress ratio $\Delta\sigma_r/\Delta\sigma_{r,max}$ in each interval has been determined for six typical relaxations, using a

graphical integration method. The obtained values are listed in table 4.

Table 4. Relaxed stress ratios for relaxations in over aged Cu-Cr-Zr at 300°C

	Dwells = 30 sec			Dwells = 300 sec		
$\Delta\varepsilon_{t\,[\%]}$ / Interval	0.413	0.82	2.014	0.41	0.825	2.02
1	0.749268	0.697866	0.698897	0.630302	0.5493663	0.557895
2	0.873929	0.842407	0.845045	0.722262	0.695324	0.663486
3	0.928101	0.917731	0.911996	0.76388	0.740792	0.713385
4	0.963998	0.965368	0.955677	0.79073	0.76996	0.745899
5	0.989452	0.986133	0.987111	0.8101196	0.791837	0.770043
6				0.835703	0.819718	0.800948
7				0.862553	0.849316	0.833141
8				0.890074	0.879771	0.866943
9				0.916924	0.908939	0.899457
10				0.945117	0.929529	0.933259
11				0.971967	0.968992	0.962774
12				0.991433	0.990868	0.989596

The time to rupture at a particular stress σ_k is taken from relation (2). Of course the relation is only supported by experimental data in the range from 185 MPa to 212 MPa. Experiments could not be run at stresses below 185 MPa because the associated rupture times would be well above one year. Therefore, for the low imposed strains, we do not have presently another choice than extrapolate relation (2) for stress values below 185 MPa. The final result is shown in figure 7 (a) for the six creep-fatigue tests run on the 3 mm specimens, at tensile dwells of 30 and 300 sec. The dependency on the strain is made clear in figure 7(b). The 300 sec dwells are the most damaging ones and the life is drastically reduced at low strain.

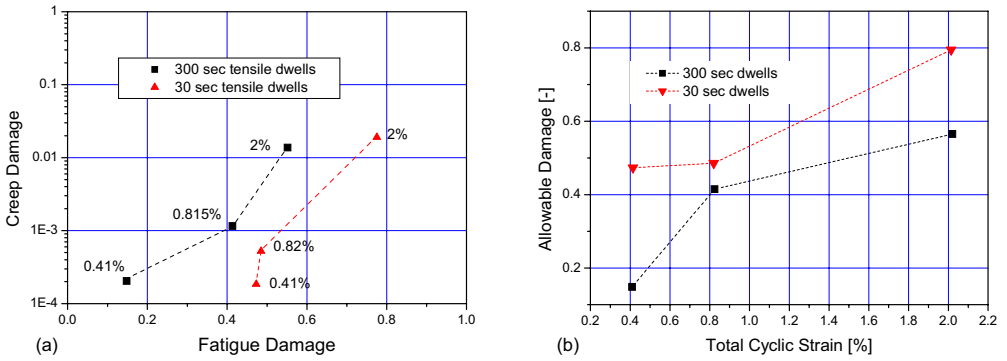

Fig. 7. (a) Damage diagram of Cu-Cr-Zr, at 300°C, for tensile dwells of 30 and 300 sec; (b) The allowable damage for creep-fatigue damage in Cu-Cr-Zr, at 300°C for tensile dwells of 30 and 300 sec. For 300 sec dwells at 0.41% total strain, the allowable damage is only about 15%.

6. Discussion

The decrease in strength after the heat treatment reported in table 2 has been well documented in the literature and is caused by modifications of the precipitated phases in the solid solution [4]. The values reported are in line with other published values [8]. The flow stress is relatively low and the material shows a strong deformation hardening in monotonic deformation, as can be deduced from the large difference between yield and ultimate stress. Due to the strong strain hardening of the soft material, the stress level observed in fatigue at low strains is lower than

the stress obtained in a creep test in tensile monotonic deformation. The associated thermal creep damage is almost negligible. This appears clearly as a result of our calculations in figure 7 (a). The thermal creep damage is negligible compared to the fatigue damage. Nevertheless the allowable damage is strongly affected and is as low as 15% at a 0.4% imposed strain with 300 sec hold time. A tentative explanation could be to argue that the reduction of life is due to increased plasticity induced by the stress relaxations. This is not true as can be seen in figure 3. The plasticity increase due to the relaxation is not large as compared to the plastic deformation already present in this soft Cu-Cr-Zr alloy. Comparison of the total stress range as a function of cycle number curves with and without hold time indicates no difference up to the point of rupture (see Fig. 2(b)). The mechanical response of the material is nearly identical for both cases. The stress relaxation is logarithmic and indicates a classical deformation process of dislocations passing obstacles by thermal activation. Evidently the crack initiation occurs earlier in life when a hold time is applied. As proposed elsewhere [9], it is believed that the reduction of life is due to a different crack initiation mechanism caused by the presence of a creep component in the cyclic deformation.

Life predictions can be done by interpolation of the experimental data. As was shown in section 4.4 and in table 4, the relaxations are quite similar in shape. Values at intermediate strains can be determined by linear interpolation. A prediction of the allowable damage can be done, applying the reverse set of calculations presented in section 5. The time base approach assumes that the creep and fatigue damage per cycle are constant over life, which has to be verified. Power equations, if used to cover a physical behaviour over many order of magnitude are quite dangerous and can give results affected by a large imprecision. Extrapolations over large ranges are dangerous. Therefore a reinforcement of the database is recommended to obtain reliable predictions over a wide parameter field.

7. Conclusions

Creep, fatigue and creep fatigue tests have been carried out at 300°C on an over aged Cu-Cr-Zr alloy. The results indicate a strong interaction between fatigue and creep. The introduction of tensile hold times reduces significantly the fatigue life of the material, the effect being larger for longer tensile dwells and for low imposed strains. The effect seems to be connected to a different crack nucleation mechanism in the presence of a creep component.

The results have been analyzed according to a time based damage assessment method. Two damage envelopes for 30 sec and 300 sec dwells have been obtained. They can be used to make life predictions between closed experimental data points.

References

[1] Bretherton, I., et al., The mechanical properties of two copper alloys: final report. 2001, AEA Technology plc: Warrington.

[2] Li, M. and J.F. Stubbins. Creep-Fatigue Behavior in High Strength Copper Alloys. in 22nd International ASTM Symposium. 2005. West Conshohocken: ASTM International.

[3] Marmy, P. and T. Kruml, Low Cycle Fatigue of Eurofer 97. J. Nucl. Mater., 2008. 377: p. 52-58.

[4] Holzwarth, U. and H. Stamm, The precipitation behaviour of ITER-grade Cu-Cr-Zr alloy after simulating the thermal cycle of isostatic pressing. Journal of Nuclear Materials, 2000. 279: p. 31-45.

[5] Feltham, P., Stress relaxation in copper and alpha brasses at low temperatures. J. Inst. Metals, 1960. 89: p. 210.

[6] Conway, J.B., R.H. Stentz, and J.T. Berling, Fatigue, Tensile and Relaxation Behavior of Stainless Steels. 1975, U. S. Atomic Energy Commission.

[7] RCC-MR, Règles de conception et de construction des matériels mécaniques des ilots nucléaires RNR. AFCEN ed. Vol. Tomes I et II. 1993.

[8] Ivanov, A.D., et al., Effect of heat treatments on the properties of Cu-Cr-Zr alloys. Journal of Nuclear Materials, 2002. 307-311: p. 673-676.

[9] Wu, X., et al., Hold-time effects on the fatigue life of Cu-Cr-Zr alloys for fusion applications. Journal of Nuclear Materials, 2007. 367-370: p. 984-989.